R-Domain Interactions with Distal Regions of CFTR Lead to Phosphorylation and Activation†

S. A. King and E. J. Sorscher*

Department of Physiology and Biophysics, Department of Medicine, University of Alabama at Birmingham, Birmingham, Alabama 35294-0005

Received December 7, 1999; Revised Manuscript Received May 9, 2000

ABSTRACT: Cystic fibrosis is caused by the aberrant function of the cystic fibrosis transmembrane conductance regulator (CFTR) protein. We examined whether intramolecular binding interactions involving the regulatory (R) domain contributed to CFTR regulation and function. When the R-domain (amino acids 596−836) was coexpressed with Δ1−836 CFTR (a carboxyl hemi-CFTR beginning immediately after the R-domain), strong binding between the two polypeptides was exhibited. The R-domain that co-immunoprecipitated with Δ1−836 exhibited a slower mobility on SDS−PAGE that resulted from phosphorylation of the protein. A larger CFTR polypeptide that included the R-domain (M837X) also exhibited a phosphorylation-dependent mobility shift when coexpressed with Δ1−836. Moreover, coexpression of M837X and Δ1−836 led to enhanced halide permeability in living cells. The activity, unlike in full-length CFTR, was present without forskolin activation, but still sensitive to the PKA inhibitor, Rp-8-CPT-cAMPS. This PKA inhibition of activity was found to be dependent on the carboxy region of the R-domain, amino acids 723−836. Our results indicate that the R-domain binds CFTR residues after amino acid 836 and that this binding facilitates phosphorylation and CFTR activation. We have also characterized a subdomain within CFTR (residues 723−837) that is necessary for PKA-dependent constitutive activation. Finally, these experiments demonstrate that constitutive CFTR activity can be accomplished by at least two mechanisms: (1) direct modulation of the R-domain to abrogate PKA regulation and (2) modifications that increase R-domain susceptibility to steady-state phosphorylation through PKA.

Cystic fibrosis (CF)[1] is a recessive genetic disease caused by abnormal function of the cystic fibrosis transmembrane conductance regulator (CFTR) protein (*1*, *2*). CFTR is a member of the ATP binding cassette (ABC) gene family, and is composed of domains characteristic of the gene family, including transmembrane domains (TMDs) and nucleotide binding domains (NBDs) (*3*). Many prokaryotic members of this family are translated as discrete polypeptides that self-assemble through multiple binding interactions to form a functional protein complex. Domain interactions within ABC proteins, therefore, form the basis of both assembly and function (*4*, *5*). In the histidine permease, for example, two NBDs (His P) must bind to the hydrophobic domains, His Q and His M, to form a membrane protein capable of histidine transport (*6*). The NBD region of the maltose permease (Mal K) must interact with another domain (Mal F) to hydrolyze ATP (*7*).

CFTR is composed of a repeated sequence of two domains common to ABC proteins: a TMD followed by a NBD (*8*). CFTR also contains a domain unique among ABC transporters, the regulatory domain (R-domain, amino acids 590−830) which divides the two TMD−NBD sequences. The R-domain contains consensus sites for cyclic AMP-dependent protein kinase A (PKA) phosphorylation. CFTR functions as a chloride channel in the epithelial membrane of several organs (*3*), and stimulation by PKA results in R-domain phosphorylation and CFTR chloride channel activation (*9*, *10*). The mechanism by which phosphorylation of the R-domain leads to channel activity is not well understood.

The R-domain contains at least nine PKA consensus sites, several of which have been shown to augment function upon phosphorylation (serines at amino acids 660, 670, 700, 737,

† This work was funded by NIH-NIDDK P50 Grant DK53090 (SCOR) and the CF Foundation R464 (RDP).

* To whom correspondence should be addressed: Director, Gregory Fleming James Cystic Fibrosis Research Center, University of Alabama at Birmingham, 1918 University Blvd. (796 MCLM), Birmingham, AL 35294-0005. Phone: (205) 934-9640. Fax: (205) 934-7593. E-mail: Sorscher@phybio.bhs.uab.edu.

[1] Abbreviations: CF, cystic fibrosis; CFTR, cystic fibrosis transmembrane conductance regulator; ABC, ATP binding cassette; NBD, nucleotide binding domain; TMD, transmembrane domain; R-domain, regulatory domain; PKA, cyclic AMP-dependent protein kinase A; His P, NBD of histidine permease; His Q and His M, TMDs of histidine permease; Mal K, NBD region of the maltose transport system; Mal F, integral membrane protein of the maltose transport system; AMP, adenosine monophosphate; ΔR-CFTR, CFTR lacking amino acids 708−835; SDS−PAGE, sodium dodecyl sulfate−polyacrylamide gel electrophoresis; DMEM, Dulbecco's Modified Eagle's Medium; FBS, fetal bovine serum; vTF7.3, vaccina virus encoding the T7 polymerase; MOI, multiplicity of infection; DOC, deoxycholic acid; PVDF, poly(vinylidene difluoride); NBT, 4-nitroblue tetrazolium chloride; SPQ, 6-methoxy-*N*-(3-sulfopropyl)quinolonium; BCIP, 5-bromo-4-chloro-3-indolyl phosphate; β-gal, β-galactosidase; Δ1−836, carboxy hemi-CFTR beginning immediately after the R-domain; M837X, CFTR truncation that ends at CFTR position 836, after the R-domain; G723X, CFTR truncation ending at residue 722 within the R-domain; K593X, CFTR truncation ending immediately before the R-domain at position 592.

10.1021/bi992807d CCC: $19.00
Published on Web 07/15/2000

795, and 813) (*11*, *12*). In previous studies, cell-free phosphorylation of isolated, purified R-domain peptide by PKA conferred a conformational change and a mobility shift of the protein as detected by SDS−PAGE (*13*). Circular dichroism studies have also demonstrated that phosphorylation changes the conformation of the purified, recombinant R-domain, causing this domain to assume a less α-helical structure (*14*). Whether the same change occurs in living cells is unknown. Past experiments demonstrated that CFTR missing amino acids 708−835 (ΔR-CFTR) led to PKA-independent activity, indicating that this region of the R-domain encodes residues necessary for PKA-dependent activation (*15*, *16*). Removal of additional portions of the R-domain (i.e., amino acids 681−835) eliminated all activity, suggesting that the amino-terminal region of the R-domain (amino acids 681−708) is necessary for chloride channel activity. Enhanced PKA-independent CFTR activity has also been achieved through replacement of PKA-targeted serines with negatively charged aspartic acid residues (*17*). Whether activation in these experiments results from changes in net charge distribution or charge-induced conformational changes is not clear. Cotten et al. recently demonstrated that sulfhydryl modification of a cysteine within the C-terminal portion of the R-domain led to augmented CFTR activity following PKA stimulation. These results may suggest that conformational changes alone (without charge manipulation) can modulate R-domain regulatory function (*18*).

Recent reports have suggested a new level of complexity in the mechanism by which the R-domain regulates CFTR, and that the R-domain does not simply mediate PKA-reversible CFTR inhibition. In studies by Ma et al. and Winters et al., the unphosphorylated R-domain expressed in trans with CFTR lacking the R-domain (ΔR-CFTR) did not inhibit function. Moreover, phosphorylation of the isolated R-domain in this setting actually increased the chloride transport activity of ΔR-CFTR, suggesting that the R-domain may interact with other domains within CFTR to enhance activity (*19*, *20*). These studies highlight the complexity of R-domain regulation of CFTR. Understanding the regions of the R-domain responsible for modulating conformational changes following phosphorylation and the relationship of R-domain modification to channel activity may help elucidate the role of this unusual domain among members of the ABC gene family.

In the study presented here, we investigated the biochemical mechanics of R-domain phosphorylation in living cells, and the binding relationships between the R-domain and other regions within CFTR. In particular, we asked the following questions. (1) Which regions of the R-domain are necessary for a mobility shift on SDS−PAGE upon phosphorylation? (2) Does the R-domain bind to other domains within CFTR? (3) Does this binding influence the phosphorylation of the R-domain? (4) Is PKA-dependent activation of CFTR modulated by regions within the protein in addition to the regulatory domain?

EXPERIMENTAL PROCEDURES

Plasmid Construction. All plasmids used in these experiments were based on pTM1, a plasmid in which the T7 RNA polymerase promoter regulates expression of inserted genes. The pTM-CFTR has been previously described (*21*). pTM-M837X was produced by amplifying a segment of CFTR with a primer encoding nucleotides 1562−1585 (including the unique *Sph*I restriction site) and a reverse primer containing nucleotides 2495−2529 (including a stop codon at residue 2515 followed by a *Stu*I site). The resulting product was inserted between the *Sph*I and *Stu*I sites of pTM-CFTR, to place a premature stop codon in place of CFTR amino acid 837. pTM-G723X was constructed using a similar strategy but with a stop codon in place of the glycine at residue 723. The pTM-R-domain was obtained using a PCR product to engineer a start site at methionine 596 and the stop site from pTM-M837X (leading to a vector expressing the R-domain protein, i.e., amino acids 596−837). pTM-Δ1−836 was cloned with PCR amplification by inserting a *Nco*I site at methionine 836. The reverse primer (from CFTR 2925 to 2955) included the *Acc*I site in CFTR followed by an engineered *Spe*I site. The *Nco*I to *Spe*I PCR product was then ligated into pTM1. This new plasmid was opened with *Acc*I, and a fragment of CFTR (from nucleotide 2935 to beyond the stop codon) was inserted to produce pTM-Δ1−836, a plasmid encoding all of CFTR after residue 836. All constructs (see Table 1) were verified by restriction endonuclease digestion and by nucleotide sequence analysis of key mutations and PCR-generated segments used in ligations.

Table 1: Summary of CFTR Constructs

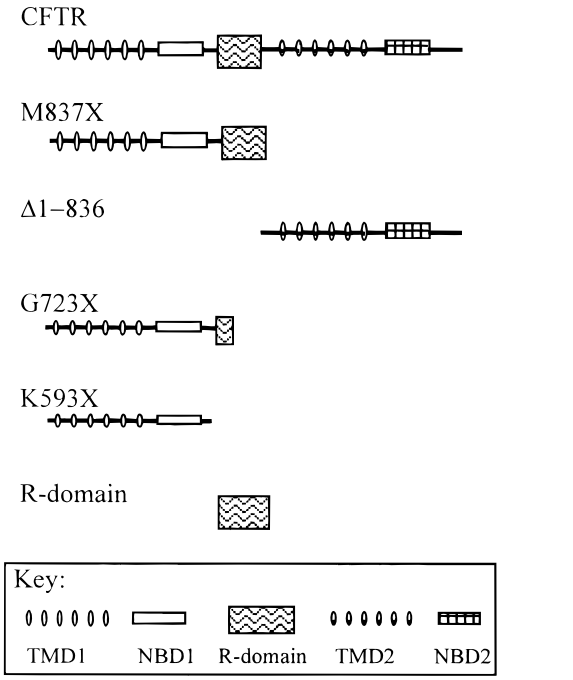

Immunoprecipitation. COS7 cells were grown in DMEM with 10% FBS and 1% penicillin/streptomycin, trypsinized, and seeded into six-well plates. When the cells reached 50−70% confluence, the medium was removed and vTF7.3 vaccina virus encoding the T7 polymerase was added at an MOI of 5−10 in Opti-MEM (Gibco BRL) (*21*, *22*). One hour later, 5 μg of pTM1 plasmid expressing all or part of CFTR was mixed with 20 μg of a 1:1 DOTAP/DOPE mixture (Avanti Polar Lipids, Birmingham, AL) in Opti-MEM, and added to the cells. After 4 h, the medium was replaced with fresh DMEM and 10% FBS. After 24 h, cells were lysed with RIPA buffer [150 mM NaCl, 50 mM Tris-HCl, 1% NP-

40, 0.5% DOC, 0.1% SDS, and the protease inhibitor cocktail Complete (Boehringer Mannheim)] for at least 20 min. The lysates were then spun for 5 min at 14 000 rpm to remove debris, and the soluble fraction was incubated with protein G or A agarose for 1 h to remove nonspecific proteins binding to the beads. The precleared lysates were added to protein A beads with a polyclonal (rabbit) antibody specific to CFTR NBD1 (*22*), or protein G beads with a monoclonal antibody specific to either the C-terminal tail or the regulatory domain of CFTR (Genzyme Corp., Cambridge, MA). Three hours later, beads were pelleted and washed three times in RIPA buffer (5 min per wash). Protein sample buffer containing SDS was added; the beads were incubated at 50° C for 15 min, and the eluted proteins were studied by 8, 10, or 16% SDS−PAGE. The proteins were then transferred to PVDF membrane, and the membrane was blocked with 3% dry milk in PBS for 20 min, stained with primary antibody for 2−4 h, and then washed three times with PBS containing 0.1% Tween 20. An alkaline phosphatase-conjugated secondary antibody (Southern Research Inc., Birmingham, AL) was administered for 1 h. The blot was then washed three times with PBS and 0.1% Tween 20, and developed with 5-bromo-4-chloro-3-indolyl phosphate (BCIP) and 4-nitroblue tetrazolium chloride (NBT) in carbonate buffer (pH 8.8) (according to the manufacturer's protocol, Boehringer Mannheim). In some experiments, cells were treated with 20 μM forskolin (Calbiochem) 20 min prior to lysis to stimulate PKA activity in the cells. Removal of phosphates from immunoprecipitated proteins was performed by treatment with alkaline phosphatase (Sigma) for 1 h at 37 °C prior to SDS−PAGE.

Fluorescence Measurements of Anion Permeability. COS7 cells were seeded onto glass coverslips. When 50−70% confluent, the cells were infected, and then transfected as described above. Twelve to sixteen hours post-transfection, the coverslips were washed with PBS and loaded with 10 mM SPQ [*N*-methyoxyl(6-propyl)quinolonium, a halide sensitive, nonpermeable fluorescent dye] by hypotonic shock [50% Opti-MEM and 50% water for 10 min as previously described (*22*)]. The cells were then incubated for 5 min in an iodide solution [buffer A being 130 mM NaI, 4 mM KNO_3, 1 mM $Ca(NO_3)_2$, 1 mM $Mg(NO_3)_2$, 10 mM glucose, and 20 mM HEPES] that quenches SPQ fluorescence. Coverslips were mounted on a fluorescence microscope, and individual cellular fluorescence was monitored every 20 s. After 3 min, the iodide quenching buffer was replaced with a nitrate dequenching buffer (buffer B has 130 mM $NaNO_3$ replacing the NaI in buffer A). At 8 min, buffer B with a 20 μM forskolin/100 μM IBMX mixture was added to activate PKA in the cells. After 13 min, buffer A was returned.

To test the effect of a PKA inhibitor, the above protocol was modified so that measurements of fluorescence were limited to the last quenching step. Shortening the protocol was performed since (1) the final quenching step was found to be the most sensitive indicator of halide permeability and (2) limiting the duration of the experiment minimized washout of the inhibitor. Cells on coverslips were treated as described above except 100 μM Rp-8-CPT-cAMPS (Biolog, La Jolla, CA) (*23*), a type I specific kinase inhibitor, was added to cells for 45 min prior to the experiment. Cells were placed in buffer B (see above) and the coverslips mounted on a fluorescence microscope. Measurements of cellular fluorescence were taken every 20 s, and after approximately 1 min, buffer B was replaced with buffer A (see above).

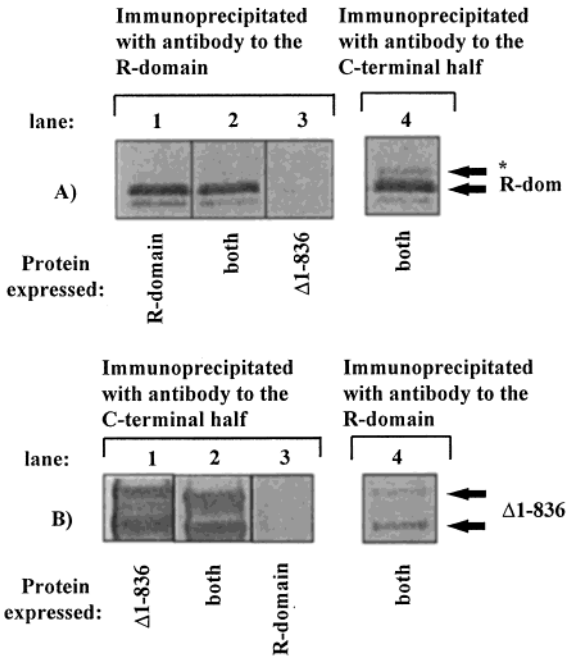

FIGURE 1: R-Domain binding to Δ1−836. The R-domain, Δ1−836, or both were expressed in COS7 cells, and immunoprecipitated proteins were studied by Western transfer. The R-domain was detected in association with Δ1−836 (panel A, lane 4, and panel B, lane 4). The asterisk denotes the shifted mobility form of the R-domain; see the text. The antibody used in Western blotting is defined on the far right side of the figure. For simplicity, the antibody used to detect Δ1−836 is called an antibody directed against the "C-terminal half" of CFTR.

RESULTS

The R-Domain Interacts with Distal CFTR Regions, and This Interaction Promotes R-Domain Phosphorylation. When the R-domain, amino acids 596−836 (Table 1), was coexpressed with Δ1−836 CFTR (the carboxyl half of CFTR beginning at amino acid 837, Table 1), a strong interaction between the two peptides could be detected (Figure 1). COS7 cells expressing either the R-domain alone, Δ1−836 alone, or the R-domain and Δ1−836 ("both") were lysed and immunoprecipitated with antibodies directed against the R-domain or Δ1−836. The R-domain, when expressed alone, could be immunoprecipitated with an antibody specific to the R-domain, but not with the C-terminal antibody. When the R-domain was coexpressed with Δ1−836, the R-domain could be co-immunoprecipitated with an antibody against the carboxy terminus of CFTR (Figure 1A, lane 4). When both proteins were expressed, Δ1−836 could also be co-immunoprecipitated with an antibody to the R-domain (Figure 1B, lane 4). The Δ1−836 construct was detected as a doublet by Western blotting (Figure 1B) as the glycosylation sites for CFTR are located within Δ1−836 (CFTR residues 894 and 900). Endo H treatment caused the collapse of the higher-molecular weight form of Δ1−836 into the lower-molecular weight nonglycosylated protein (data not shown).

A portion of the R-domain which bound to Δ1−836 also exhibited a mobility shift toward a higher apparent molecular weight (Figure 1A, lane 4 with *). Since phosphorylation of

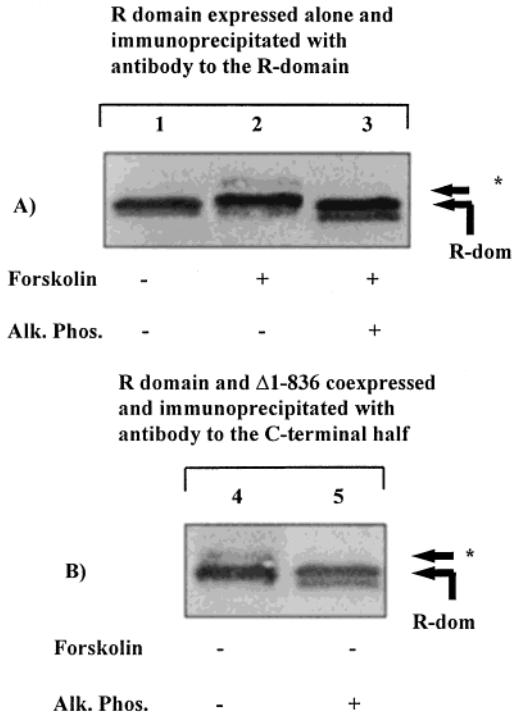

FIGURE 2: Forskolin treatment or coexpression with Δ1−836 produces an apparent higher-molecular weight R-domain protein that is sensitive to alkaline phosphatase. Immunoprecipitates from cells expressing the R-domain or the R-domain with Δ1−836 were studied as described in the legend of Figure 1. Some of the immunoprecipitated samples were incubated with alkaline phosphatase (Alk. phos.) prior to gel electrophoresis. The R-domain from cells treated with forskolin and the R-domain bound to Δ1−836 resulted in an apparent higher-molecular weight R-domain protein band (*, lanes 2 and 4). The higher-molecular weight R-domain protein band was eliminated by treatment with alkaline phosphatase (lanes 3 and 5).

the R-domain predicts a conformational change and a higher molecular weight, we carried out experiments to determine whether the shift in electrophoretic mobility was secondary to phosphorylation. Forskolin treatment of cells expressing the R-domain alone elicited a shift in R-domain migration comparable to that observed following coexpression of the R-domain with Δ1−836 (approximately 3−5 kDa, Figure 2A, lane 2). However, the addition of phosphate groups to the R-domain would not be expected to elicit a mobility shift of this size solely on the basis of molecular mass. The altered migration through SDS−PAGE, therefore, may be attributable to a less globular conformation of the R-domain elicited by phosphorylation (rather than to the addition of phosphates per se). A similar change in R-domain migration following phosphorylation has been previously reported in a cell-free system (*14*). To further confirm that phosphorylation was the cause of the shift in the apparent molecular weight, the immunoprecipitated proteins were treated with alkaline phosphatase. Dephosphorylation of the R-domain caused the collapse of the apparent higher-molecular weight protein to the lower-molecular weight form (Figure 2B, lanes 4 and 5). The results in Figures 1 and 2 therefore suggest a biochemical consequence (phosphorylation-dependent mobility shift) in living cells due to coexpression of the R-domain with Δ1−836 CFTR. To further verify the specificity of the co-immunoprecipitation of the R-domain with Δ1−836, experiments using β-galactosidase (β-gal) coexpression with either the R-domain or Δ1−836 were performed. The (β-gal) control protein was expressed at levels approximately equal to those of the recombinant CFTR polypeptides. Neither the R-domain nor Δ1−836 co-immunoprecipitated with β-gal (data not shown).

Interactions between Δ1−836 and M837X Confer Phosphorylation of the R-Domain and Activation of Halide Efflux. To ascertain whether phosphorylation of the R-domain is enhanced by expression of the complete CFTR amino acid sequence, we transfected cells with both Δ1−836 and M837X (CFTR truncated at the end of the R-domain, Table 1). Coexpression of these two portions of CFTR is equivalent to a full-length molecule that has been cleaved at residue 837. Interactions between the two halves of CFTR were demonstrated using amino- and carboxy-terminal specific antibodies. Immunoprecipitates from COS7 cells expressing M837X, Δ1−836, or both were studied by Western blotting, as shown in Figure 3. The M837X protein was pulled down in association with Δ1−836 (Figure 3A). The complementary experiment showed that Δ1−836 could also be co-immunoprecipitated in association with M837X (Figure 3B, lane 6). Neither M837X nor Δ1−836 bound to a control (β-gal) protein (Figure 3C). Interestingly, the M837X protein that co-immunoprecipitated with Δ1−836 was greatly enriched for an apparent higher-molecular weight conformation (Figure 3A, lane 4 with *). Direct immunoprecipitation of M837X indicated that the total level of shifted M837X protein was negligible when expressed alone (Figure 3A, lane 1). When M837X was coexpressed with Δ1−836, the higher protein band could be more readily detected, and was dramatically enriched bound to Δ1−836 (Figure 3A, lane 4). To test whether phosphorylation was responsible for the mobility shift in M837X, cells expressing M837X alone were treated with forskolin prior to lysis. Forskolin treatment reproduced the slower molecular weight migration in M837X (Figure 4A, lane 1). Alkaline phosphatase treatment of immunoprecipitated M837X protein abolished the higher-molecular weight band seen following either PKA stimulation or coexpression with Δ1−836 (Figure 4A, lanes 2 and 4). These results indicate that the expression of Δ1−836 with M837X confers a phosphorylation-dependent reduction in the mobility of M837X. Forskolin treatment did not cause phosphorylation of all the expressed R-domain or M837X. We speculate, therefore, that R-domain phosphorylation may be relatively restricted to certain cellular subcompartments. Previous experiments reported by our laboratory (*24*) have suggested the cellular localization of portions of the first half of CFTR may depend on several factors, including coexpression with the second half of the protein. If this were so, only a subfraction of the R-domain or M837X might be situated within the cell in a position suitable for efficient phosphorylation by PKA. Additional studies will be required to examine this possibility.

The CFTR chloride channel is activated by PKA-dependent phosphorylation of the R-domain (*9*, *10*). Since we observed that binding between M837X and Δ1−836 augments CFTR phosphorylation, we tested the functional consequences of this binding interaction. M837X, Δ1−836, or both were expressed in COS7 cells, and anion efflux was measured using the halide sensitive dye SPQ. Coexpression of M837X and Δ1−836 led to augmented cellular halide permeability (Figure 5, ●), while no halide efflux above

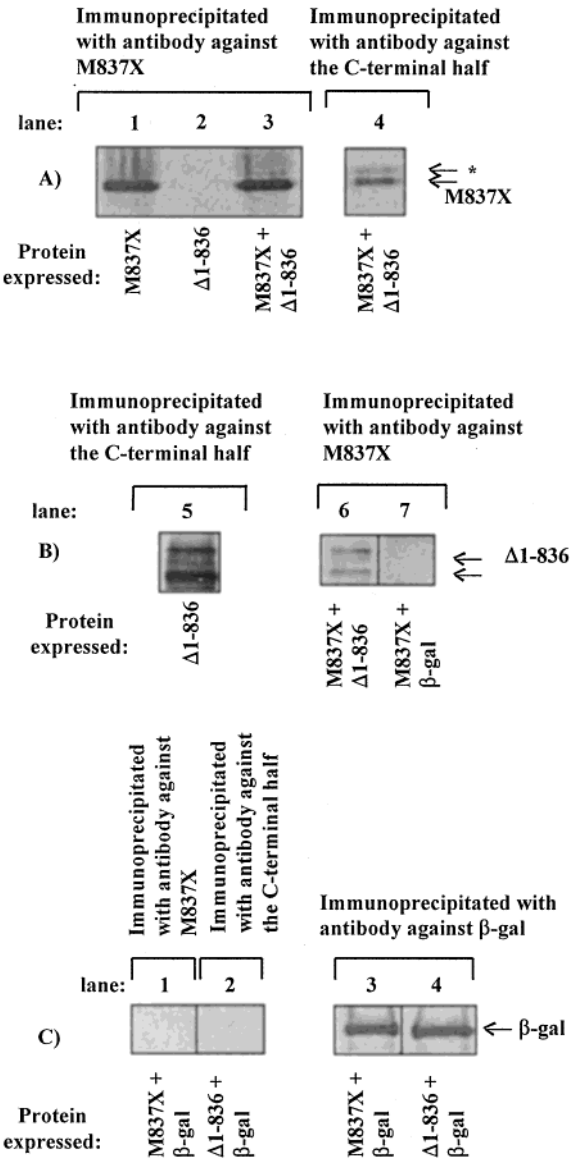

FIGURE 3: M837X binds Δ1−836. M837X, Δ1−836, or both were immunoprecipitated using an antibody specific to M837X, or to the C-terminal half. M837X co-immunoprecipitated with Δ1−836 (panel A, lane 4). The Δ1−836 was also detected following co-immunoprecipitation with M837X (panel B, lane 6). Neither portion of CFTR bound *β*-gal (panel C). The asterisk denotes the shifted mobility form of M837X; see the text. The antibody used in Western blotting is defined at the right of each panel.

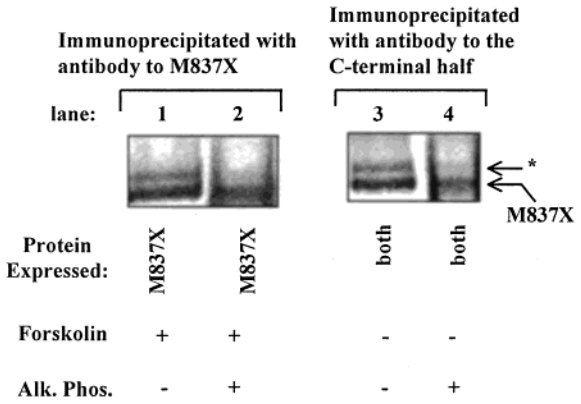

FIGURE 4: Forskolin treatment or coexpression with Δ1−836 produces an apparent higher-molecular weight, alkaline phosphatase sensitive form of M837X. Lysates from cells expressing M837X, alone or together with Δ1−836 ("both"), were immunoprecipitated as described in the legend of Figure 3. Half of the immunoprecipitated proteins were incubated with alkaline phosphatase prior to Western blotting. M837X from cells treated with forskolin and M837X coexpressed with Δ1−836 resulted in an apparent higher-molecular weight M837X-CFTR protein band (*, lanes 1 and 3). The higher-molecular weight M837X protein band was eliminated by treatment with alkaline phosphatase (lanes 2 and 4).

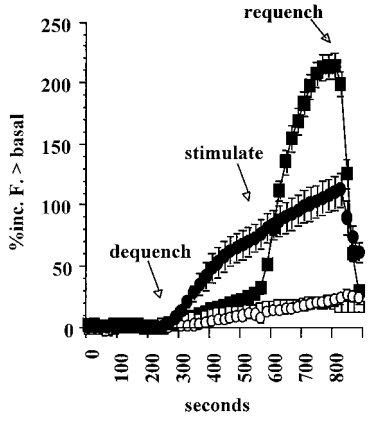

FIGURE 5: M837X and Δ1−836 coexpression produces elevated basal halide efflux. CFTR (■), M837X (□), Δ1−836 (○), or M837X and Δ1−836 (●) were expressed in COS7 cells, and halide efflux was assayed using the halide sensitive intracellular dye SPQ. The cells were bathed in an iodide buffer to quench SPQ fluorescence. Then at 200 s, the iodide buffer was replaced with nitrate buffer (dequench); at 500 s, forskolin and IBMX were added to the nitrate buffer (stimulate), and at 800 s, the iodide buffer was returned (requench). Enhanced basal halide efflux following the switch to the dequench buffer was detected in cells coexpressing M837X and Δ1−836 ($p < 0.001$), and regulated halide efflux was seen with expression of CFTR upon forskolin stimulation ($p < 0.001$). No enhanced halide movement was detected when either M837X or Δ1−836 was expressed alone. %inc. F. > basal represents the percentage increase in fluorescence above the base flourescence in quenching buffer (average between 100 and 200 s). Error bars represent the standard error of the mean. More than 250 cells were studied per condition.

background was detected in cells expressing either M837X or Δ1−836 alone (Figure 5, □ and ○). Coexpression of M837X and Δ1−836 produced predominantly constitutive function of the reconstituted CFTR, similar to that reported previously for CFTR lacking a portion of the R-domain (ΔR-CFTR) (*15*, *19*). Previous coexpression studies of the first and second halves of CFTR in eukaryotic cells have been reported to form a PKA-regulated halide channel (*25*). Unlike this previous report, the activity shown in Figure 5 was predominantly basal (with little additional response to PKA). While addition of forskolin did not produce significant increases in activity, minor increases in halide permeability could occasionally be detected, suggesting there may be differences between COS7 cells (used in these studies) and HeLa cells (used in the previous report) in the endogenous levels of PKA activity.

The increased halide efflux conferred by M837X and Δ1−836 could be either due to the loss of PKA-dependent regulation of CFTR [as demonstrated for ΔR-CFTR (*15*)] or a result of enhanced R-domain basal PKA phosphorylation. To determine the role of PKA on the basal activity, we studied the effects of PKA inhibition. When cells coexpressing M837X and Δ1−836 were treated with Rp-8-CPT-cAMPS, a PKA antagonist, a significant decrease in the halide efflux was detected compared to that in untreated cells

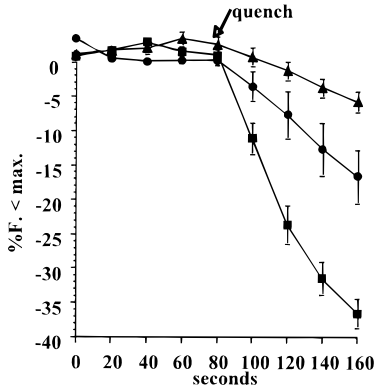

FIGURE 6: Halide permeability produced by M837X and Δ1−836 is PKA-dependent. M837X (▲) or M837X and Δ1−836 (■) were expressed in COS7 cells. Cells expressing M837X and Δ1−836 were treated with Rp-8-CPT-cAMPS (●), a PKA antagonist. Halide movement was assayed using SPQ. At 80 s, the nitrate buffer was replaced with iodide buffer, and the rate of flourescence quenching was monitored. Rp-8-CPT-cAMPS dramatically inhibited the halide permeability of M837X and Δ1−836 ($p < 0.05$). Permeability coefficients (average changes in flourescence per 20 s from 80 to 120 s) were −2.2 (M837X), −12.3 (M837X and Δ1−836), and −3.9 (M837X and Δ1−836, with Rp-8CPT-cAMPS treatment). More than 150 cells were studied per condition.

(Figure 6). These results indicate that enhanced PKA-dependent phosphorylation of M837X is responsible for the high basal halide efflux produced following coexpression of M837X and Δ1−836.

The Carboxy Region of the R-Domain Is Necessary for the Phosphorylation-Dependent M837X Mobility Shift and PKA-Dependent Halide Efflux. To examine R-domain residues that are necessary for the phosphorylation of M837X elicited by Δ1−836, we tested shortened CFTR truncations missing part or all of the R-domain for functional and biochemical interactions with Δ1−836. G723X (missing the 114 C-terminal amino acids of the R-domain, Table 1) was tested for the phosphorylation-dependent mobility shift following coexpression with Δ1−836. While G723X co-immunoprecipitated with Δ1−836 in a manner similar to that of M837X, this interaction did not result in a mobility shift of the G723X protein (Figure 7A, compare lanes 3 and 4). Furthermore, no molecular weight shift of G723X could be detected when cells were treated with forskolin prior to lysis (Figure 7B, lane 4). G723X and Δ1−836 expressed together produced constitutive (unregulated) activity (Figure 8A). However, in marked contrast to the results shown in Figure 6, this activity could not be inhibited by a PKA antagonist (Figure 8B). Additional deletion of R-domain residues produces substantial functional consequences. K593X (CFTR truncated immediately before the R-domain, Table 1) co-immunoprecipitated with Δ1−836 in a manner similar to that of M837X or G723X (data not shown), but coexpression of K593X with Δ1−836 failed to produce enhanced halide efflux (Figure 8A). These studies, therefore, demonstrate that interactions occurring between the R-domain and downstream portions of CFTR result in enhanced phosphorylation and PKA-dependent activity that is dependent on amino acids 723−837.

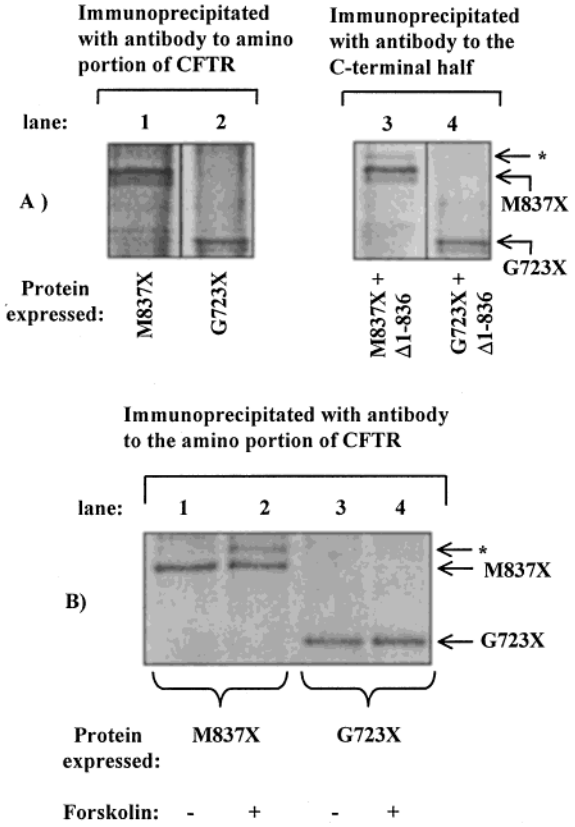

FIGURE 7: G723X binds Δ1−836, but this interaction does not elicit a mobility shift of G723X. (A) CFTR polypeptides were studied as described in the legend of Figure 3. While both G723X and M837X bind Δ1−836 (lanes 3 and 4), only the interaction of M837X with Δ1−836 produced a higher-molecular weight phosphorylated protein (*, lane 3). (B) Cells expressing M837X or G723X were treated with forskolin prior to lysis (as described in the legend of Figure 4). M837X from cells treated with forskolin appeared as an apparent higher-molecular weight M837X-CFTR protein band (*, lane 2). However, forskolin treament of cells expressing G723X did not result in a higher-molecular weight protein (lane 4).

DISCUSSION

The experiments presented here were designed to test the interaction of the regulatory domain (R-domain) of CFTR with distal regions of the protein, and to determine whether these interactions play a role in CFTR regulation. When COS7 cells expressing the CFTR R-domain (amino acids 596−837) were treated with forskolin, a mobility shift in the protein to a higher apparent molecular weight was observed (Figure 2). The shift was due to phosphorylation, and could be eliminated by alkaline phosphatase treatment. When the R-domain was coexpressed with downstream elements of CFTR (residues 836−1480), physical binding between these two portions of CFTR was established by co-immunoprecipitation (Figure 1). Coexpression of Δ1−836 with the R-domain also conferred a mobility shift of the R-domain on SDS−PAGE that was very similar to that observed with the R-domain alone following treatment with forskolin, and was again abrogated by alkaline phosphatase. Enhanced phosphorylation of the R-domain was also observed when the first half of CFTR, M837X (CFTR truncated immediately after the R-domain), was treated with forskolin or coexpressed with Δ1−836. These results therefore indicate that the R-domain binds to distal regions of CFTR, and this binding has biochemical consequences (Figures 1−4). A shorter amino truncation (G723X) also tightly bound to Δ1−836. In contrast to M837X, G723X failed to exhibit a reduced mobility on SDS−PAGE after either coexpression with Δ1−

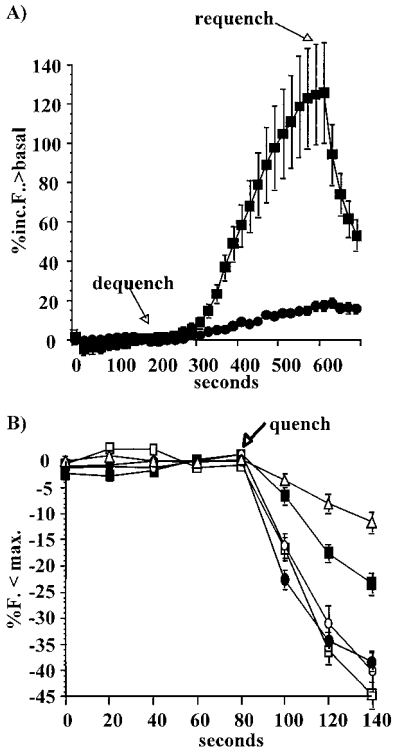

FIGURE 8: G723X coexpression with Δ1−836 produces enhanced halide efflux, while K593X does not. (A) G723X and Δ1−836 (■) or K593X and Δ1−836 (●) were expressed in COS7 cells, and halide efflux was assayed as described in the legend of Figure 5. G723X produced high basal halide permeability when coexpressed with Δ1−836 ($p < 0.01$) similar to that of M837X with Δ1−836 (Figure 5). K593X, missing the complete R-domain, failed to increase halide permeability when coexpressed with Δ1−836. Stimulation with forskolin had no effect on halide permeability for either condition (data not shown). More than 150 cells were studied per condition. (B) M837X and Δ1−836 (□) or G723X and Δ1−836 (○) were expressed in COS7 cells and assayed for halide movement as described in the legend of Figure 6. Rp-8-CPT-cAMPS inhibited the enhanced halide permeability of M837X and Δ1−836 (■, $p < 0.05$), but not that of G723X and Δ1−836 (●). (△) Negative control with T7 polymerase (no CFTR).

836 or forskolin treatment (Figure 7). This result demonstrates the importance of the last 114 amino acids of the R-domain in the phosphorylation-dependent mobility shift of the R-domain (Figures 1−4 and 7).

Intramolecular interactions within CFTR have been described previously between the two membrane-spanning domains of CFTR (*25*). The experiments presented here establish that binding also occurs between the R-domain and other regions of CFTR, and that this binding has functional consequences. M837X coexpressed with Δ1−836 resulted in high-level CFTR activity (as detected by SPQ, Figure 5) in the absence of additional PKA stimulation, indicating that R-domain interactions with downstream domains can augment R-domain phosphorylation and directly regulate CFTR function. High-level, PKA-independent activity has been reported for a CFTR lacking amino acids 708−835 of the R-domain (ΔR-CFTR). In contrast to ΔR-CFTR, the basal activity of M837X with Δ1−836 reported in this study was PKA-dependent, and could be inhibited by the PKA antagonist Rp-8-CPT-cAMPS. Therefore, while ΔR-CFTR functions independently of PKA, the high basal activity conferred by coexpression of M837X with Δ1−836 results from a different, phosphorylation-dependent mechanism. G723X also produced high basal halide efflux when it was coexpressed with Δ1−836 (Figure 8A). However, in contrast to M837X, the activity could not be inhibited by PKA antagonists (Figure 8B), a result similar to the activity reported for ΔR-CFTR. On the basis of the observations that (1) the level of the phosphorylation-dependent higher-molecular weight M837X was dramatically increased when it was bound to Δ1−836, (2) a high basal halide permeability was produced by coexpression of M837X with Δ1−836, and (3) this activity was suppressed by PKA inhibitors, we conclude that R-domain phosphorylation and CFTR activation were promoted by R-domain interactions with downstream elements of CFTR. The increased susceptibility of the R-domain to PKA phosphorylation in the two-subunit model of CFTR (M837X and Δ1−836) may reflect greater accessibility of the R-domain to endogenous PKA, or blockade of phosphatase action. In either case, the results presented here offer a means by which R-domain function in living cells can be monitored biochemically, and mutations that disrupt PKA regulation of CFTR can be better characterized.

Although the R-domain has been defined as a single discrete domain derived from CFTR exon 13, Dulhanty and Riordan suggested that the R-domain might be divided into two functionally distinct subregions, RD1 (amino acids 587−672) and RD2 (amino acids 679−798) (*26*). The amino-terminal third of the R-domain, RD1, appears to be necessary for chloride channel function. This region exhibits strong homology between CFTRs from several different species, and also exhibits sequence homology to the linker region of another ABC polypeptide, the multidrug resistant (MDR) protein. In this study, we show that the carboxy-terminal portion of the R-domain (RD2), while not necessary for channel activity, plays a critical role in CFTR inhibition under basal conditions. If the carboxy terminus of the R-domain (the last 114 amino acids) is omitted, PKA-dependent activation is lost, although channel activity is readily detected. This portion of the R-domain is therefore required to biochemically alter the structure of the R-domain upon phosphorylation in cells, and is likely to comprise the "switch" regulating initial PKA-dependent CFTR activation. Recent experiments have illustrated binding of the amino portion of the R-domain to the amino tail of CFTR (*27*). Naren et al. demonstrated the importance of this interaction in maintaining an open state conformation. R-Domain interactions therefore subserve complex regulatory functions that contribute to both initial (PKA-dependent) activation and subsequent maintenance of the CFTR open state.

In summary, the study presented here provides new biochemical evidence for a PKA-dependent structural change in the R-domain as a direct result of phosphorylation in living cells. This change correlates with CFTR activation, and is strongly facilitated by binding between the R-domain and CFTR residues after amino acid 836. Moreover, we have characterized a subdomain within the regulatory domain of CFTR (residues 723−837) that is necessary for PKA-dependent activation. Finally, these experiments demonstrate that constitutive CFTR activity can be accomplished by at least two mechanisms: (1) direct modulation of the R-domain (by serine mutations or partial R-domain deletions) or (2) enhanced susceptibility of CFTR to steady-state PKA phosphorylation.

ACKNOWLEDGMENT

We thank Drs. Kevin Kirk, Dale Benos, Doug Cyr, and Jim Collawn for useful discussion and review. We are also in debt to Drs. J. P. Clancy, A. P. Naren, Z. Bebok, and J. Hong for reviewing the manuscript and Kynda Roberts for help in manuscript preparation.

REFERENCES

1. Cheng, S. H., Gregory, R. J., Marshall, J., Paul, S., Souza, D. W., White, G. A., O'Riordan, C. R., and Smith, A. E. (1990) *Cell 63*, 827−834.
2. Rich, D. P., Anderson, M. P., Gregory, R. J., Cheng, S. H., Paul, S., Jefferson, D. M., McCann, J. D., Klinger, K. W., Smith, A. E., et al. (1990) *Nature 347*, 358−363.
3. Hyde, S. C., Emsley, P., Hartshorn, M. J., Mimmack, M. M., Gileadi, U., Pearce, S. R., Gallagher, M. P., Gill, D. R., Hubbard, R. E., et al. (1990) *Nature 346*, 362−365.
4. Loo, T. W., and Clarke, D. M. (1995) *J. Biol. Chem. 270*, 21839−21844.
5. Schneider, E., and Hunke, S. (1998) *FEMS Microbiol. Rev. 22*, 1−20.
6. Ames, G. F., Mimura, C. S., Holbrook, S. R., and Shyamala, V. (1992) *Adv . Enzymol. Relat. Areas Mol. Biol. 65*, 1−47.
7. Panagiotidis, C. H., Reyes, M., Sievertsen, A., Boos, W., and Shuman, H. A. (1993) *J. Biol. Chem. 268*, 23685−23696.
8. Riordan, J. R., Rommens, J. M., Kerem, B., Alon, N., Rozmahel, R., Grzelczak, Z., Zielenski, J., Lok, S., Plavsic, N., et al. (1989) *Science 245*, 1066−1073.
9. Anderson, M. P., Berger, H. A., Rich, D. P., Gregory, R. J., Smith, A. E., and Welsh, M. J. (1991) *Cell 67*, 775−784.
10. Fuller, C. M., and Benos, D. J. (1992) *Am. J. Physiol. 263*, C267−C286.
11. Cheng, S. H., Rich, D. P., Marshall, J., Gregory, R. J., Welsh, M. J., and Smith, A. E. (1991) *Cell 66*, 1027−1036.
12. Wilkinson, D., Strong, T., Mansoura, M., Wood, D., Smith, S., Collins, F., and Dawson, D. (1997) *Am. J. Physiol. 273*, L127−L133.
13. Picciotto, M. R., Cohn, J. A., Bertuzzi, G., Greengard, P., and Nairn, A. C. (1992) *J. Biol. Chem. 267*, 12742−12752.
14. Dulhanty, A. M., and Riordan, J. R. (1994) *Biochemistry 33*, 4072−4079.
15. Rich, D. P., Gregory, R. J., Anderson, M. P., Manavalan, P., Smith, A. E., and Welsh, M. J. (1991) *Science 253*, 205−207.
16. Rich, D. P., Gregory, R. J., Cheng, S. H., Smith, A. E., and Welsh, M. J. (1993) *Recept. Channels 1*, 221−232.
17. Rich, D. P., Berger, H. A., Cheng, S. H., Travis, S. M., Saxena, M., Smith, A. E., and Welsh, M. J. (1993) *J. Biol. Chem. 268*, 20259−20267.
18. Cotten, J. F., and Welsh, M. J. (1997) *J. Biol. Chem. 272*, 25617−25622.
19. Ma, J., Zhao, J., Drumm, M. L., Xie, J., and Davis, P. B. (1997) *J. Biol. Chem. 272*, 28133−28141.
20. Winter, M. C., and Welsh, M. J. (1997) *Nature 389*, 294−296.
21. Walker, L. C., Venglarik, C. J., Aubin, G., Weatherly, M. R., McCarty, N. A., Lesnick, B., Ruiz, F., Clancy, J. P., and Sorscher, E. J. (1997) *Am. J. Respir. Crit. Care Med. 155*, 1684−1689.
22. Clancy, J. P., et al. (1998) *Biochemistry 37*, 15222−15230.
23. Gjertsen, B. T., et al. (1995) *J. Biol. Chem. 270*, 20599−20607.
24. King, S. A., and Sorscher, E. J. (1997) *Ped. Pulmon. Suppl. 17*, 21.
25. Ostedgaard, L. S., Rich, D. P., DeBerg, L. G., and Welsh, M. J. (1997) *Biochemistry 36*, 1287−1294.
26. Dulhanty, A. M., and Riordan, J. R. (1994) *FEBS Lett. 343*, 109−114.
27. Naren, A. P., Cormet-Boyaka, E., Fu, J., Villain, M., Blalock, J. E., Quick, M. W., and Kirk, K. L. (1999) *Science 286*, 544−548.

BI992807D